BioMOCA: a Transport Monte Carlo Approach to Ion Channel Simulation

T.A. van der Straaten, G. Kathawala, U. Ravaioli

Beckman Institute for Advanced Science and Technology,
University of Illinois, Urbana, IL 61801, USA
trudyv@uiuc.edu, gkathawa@uiuc.edu, ravaioli@uiuc.edu

ABSTRACT

Ion channels are highly charged proteins that reside in the membrane of all living cells to regulate charge transport to the cell. Most channels have device-like behaviors that are interesting to the electronics community for their possible application in bio-device design. Simulating ion channels over time-scales relevant to conduction present a difficult time and space multi-scale problem that is beyond the scope of the Molecular Dynamics approach. To address this problem we have developed BioMOCA, a 3-D reduced particle ion channel simulator based on the transport Monte Carlo methodology. BioMOCA has been described elsewhere; here we use it to study the link between the electrostatic properties of the protein and selectivity in the *gramicidin* channel. We also present representative simulations of Na^+ transport in *gramicidin*.

Keywords: ion channels, nanodevices, gramicidin, Monte Carlo simulations

1 INTRODUCTION

Ion channels are proteins that fold in such a way that they form natural conducting nanopores spanning the membranes of biological cells, thereby controlling the ion transport in and out of the cell. The side-chains of the amino acids are ionizable resulting in a strong permanent charge that varies sharply along the surface of the protein. Many channels can selectively transmit or block a particular ion species, and most have switching properties or perform specialized functions resembling those of complex electronic systems [1]. The device-like behaviors exhibited by ion channels intrigue the engineering community for many reasons. Ion channels have the distinct advantage of perfect structure duplication and self-assembly, while solid-state nanoscale device counterparts tend to be strongly affected by statistical fluctuations and defects. Channel mutation, which involves replacing or deleting one or more amino acids, allows the channel structure and charge distribution to be controlled in the laboratory with atomic resolution [2,3]. Engineering of natural channels, with specific conductance and selectivity properties, is thus conceivable.

Simulations can help provide a clearer understanding of channel operation. However, the simulation of ion channels embedded in a macroscopic membrane environment is a formidable multi-scale problem in both time and space. Channel/membrane system dimensions range from ~10nm to ~1μm, while specific channel functions, such as switching or selectivity, are often controlled by sub-nm functional sub-units of the protein. Thus, at least part of the channel system needs to be represented with atomic resolution. In addition, ion traversal through the channel is a rare event, so ion motion must be resolved on a fs scale. On the other hand, reliable estimates of current require simulations lasting several ~μs. Realistic simulations are also difficult because at present the complete molecular structure and charge distribution is known from measurements for only a few channels. Even then, it is difficult to predict the structural and electrostatic changes that may occur when the channel is exposed to different physiological conditions.

With the advent of standardized software and massively parallel computing power, Molecular Dynamics (MD) [4] has become the most widely employed tool for studying ion dynamics in protein channels [5]. Although MD simulations can provide key information regarding the mechanisms of ion conduction in atomic detail, the resources required to compute steady-state channel currents directly using this approach well exceed the most powerful machines currently available. At the other end of the simulation hierarchy, continuum models based on drift-diffusion theory can be used to compute macroscopic currents quickly [6-8]. However, ion diffusivities and dielectric coefficients must be assigned with some care since the continuum paradigm deals with average densities rather than discrete particles of finite size, a premise that has been found to overestimate the ion concentration in very narrow channels.

In order to extend simulation times to ~μs, while still retaining some atomic level of detail, we have developed BioMOCA, a 3-D reduced particle ion channel simulator based on the Monte Carlo methodology developed for charge carrier transport in solid-state devices. Since BioMOCA has been described in detail elsewhere [9,10], we give only a brief overview. Water, protein and lipid membrane are treated as continuum dielectric media while ions are modeled as discrete finite-sized particles. Ion trajectories are traced in real space as sequences of free flights randomly interrupted by thermalizing scattering events that represent the interaction between ions and the surrounding channel/electrolyte environment. The duration of free flights is linked to the ion's diffusivity in the electrolyte. Ion size is modeled by dressing the ions with a pairwise Lennard-Jones potential and electrostatic forces

are calculated self-consistently from the charged particles positions by solving Poisson's equation.

In the following section we discuss the electrostatic properties of ion channels, and the role this plays in the observed cation selectivity of the *gramicidin* (gA) channel. In section 3 we compare BioMOCA simulations of gramicidin with a 3-D continuum simulation. We also conducted BioMOCA simulations of the *porin* ion channel but because of space limitations these results are not discussed here.

2 GRAMICIDIN: PROPERTIES

Gramicidin A (gA) is a small channel-forming molecule consisting of 15 amino acids folded into a helical structure. When two gA molecules align end-to-end creating a dimer, a narrow channel (~25Å long, ~4Å in diameter) is formed spanning the membrane. Although it is charge-neutral overall, the charge distribution on the mouth of the gA channel and lining the pore imparts a signature double well electrostatic potential profile. gA only conducts small monovalent cations; anions are completely excluded from the channel

The issue of what permittivity values ε_p to assign to protein has been addressed in several recent articles (see [11] and references within). The protein environment can respond to an external field in several ways, each with its own relaxation time, e.g., field-induced dipoles, re-orientation of permanent dipoles and larger scale re-organization of ionized side-chains and water molecules, both within the interior and on the surface of the protein. In deciding what value to assign to ε_p one must consider how much physics is included explicitly. If all of the charges and dipoles are included explicitly, as in MD simulations, then clearly $\varepsilon = 1$ everywhere. If all but the field-induced atomic polarization is treated explicitly then $\varepsilon_p \sim 2$. However, when protein and water re-organization are included implicitly the dielectric coefficient is hard to define, particularly when ion motion takes place on the same time-scale as the protein's response to its presence. It has been suggested that for continuum models that seek to encapsulate the dielectric response of the water and protein side-chains with a dielectric coefficient, the value of ε_p should be significantly larger than 2 [11].

In gA the channel is also lined with dipoles formed by negatively charged carbonyls and positively charged amino groups, which hydrogen-bond to each other, helping to stabilize the helical structure. The dipoles are tilted with respected to the channel axis such that the carbonyls protrude slightly into the pore. MD simulations have shown that these carbonyls also form hydrogen bonds with water molecules that, due to the narrow width of the pore, must traverse the channel in single file [12]. As a result, water is highly ordered within the channel so the dielectric coefficient of the aqueous pore (ε_c) should really be much lower than the value of 80 used for water under bulk conditions. Nonetheless, in their attempts to explain gA's

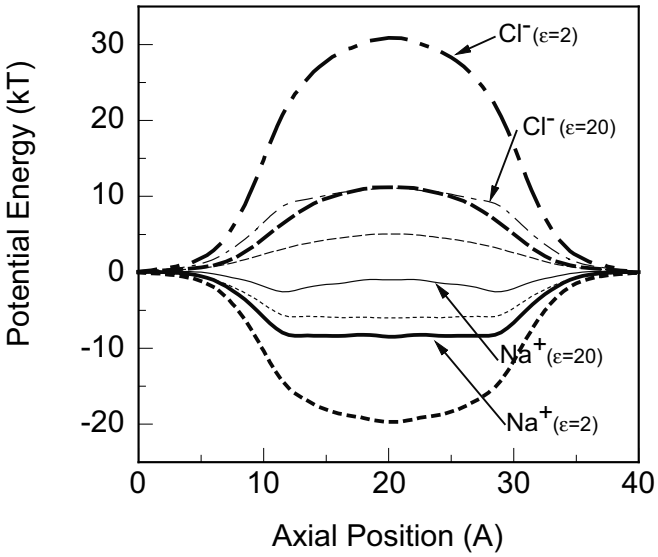

Figure 1 Net PE profiles seen by Na^+(solid lines) and Cl^- (dash-dot) ions traversing the center of gA. The individual contributions from the partial charges (short dash) and the dielectric barrier (long dash) are also shown. Thick lines indicate $\varepsilon_p = 2$, fine lines indicate $\varepsilon_p = 20$.

monovalent cation selectivity, several groups have assumed $\varepsilon_{ch} = 80$. For comparison, the results presented in this section were also obtained using $\varepsilon_{ch} = 80$.

Recently it has been proposed [13,14] that the mechanism allowing gA to conduct monovalent cations while blocking anions and divalent ions lies in the permanent charge being distributed over the protein in such a way that it creates a potential well for cations, that cancels the potential barrier created by the low dielectric ($\varepsilon_p = 2$) protein environment. Figure 1 shows the net potential energy (PE) profile seen by a single Na^+ ion traversing the center of a gA channel embedded in a low dielectric slab representative of the lipid membrane. The individual contributions from the partial charges and the dielectric barrier are also shown. These profiles were computed with BioMOCA, using the 1mag.pdb structure and the partial charges used by Edwards et al. [13] (PARAM22 version of CHARMM force field]). The dielectric coefficients of protein and lipid were set to 2, while the aqueous interior of the channel and electrolyte baths were given $\varepsilon_{water} = 80$. The large barrier $\sim 10 k_B T$ created by the protein dielectric is more than cancelled by the deep potential well $\sim 19 k_B T$ created by the permanent charge on the protein, allowing Na^+ conduction through the pore. In contrast, since the PE barrier caused by the dielectric is independent of the sign of the charge, and the permanent charges present an additional barrier to negative ions, the corresponding net PE profile for Cl^- shows a $\sim 30 k_B T$ barrier that would prevent Cl^- from entering the channel. Thus, if a low protein dielectric coefficient is used, the cancellation of permanent charge and dielectric barrier is a valid explanation for cation selectivity. However, as discussed above, 2 may not be a

reasonable value for ε_p. Also shown in Figure 1 are the Na^+ and Cl^- profiles computed using ε_p = 20. In this case, the potential barrier due to the protein dielectric and the potential well due to the partial charges become much smaller. The cancellation of dielectric barrier and the potential well due to the partial charges still holds for Na^+ but the net barrier for Cl^- is now much lower (~11k_BT). Under an applied bias of 250 mV (~10k_BT) it may be possible for Cl^- to enter the channel. Thus it is not clear whether the explanation for gA cation selectivity in [13,14] holds unless a very low protein dielectric coefficient is assumed. Further, in the next section we show that alternative data for the permanent charge distribution can produce a sizeable potential barrier for the Na^+ that can still be overcome under an applied bias.

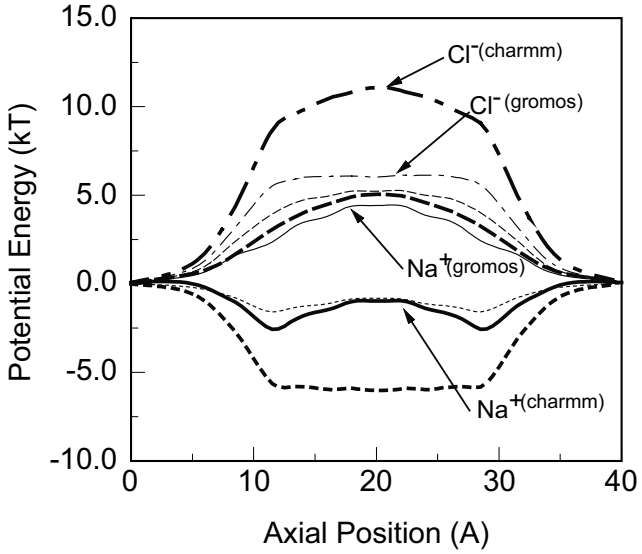

Figure 2 Net PE profiles seen by Na^+(solid lines) and Cl^- (dash-dot) ions traversing the center of gA. The individual contributions from the partial charges (short dash) and the dielectric barrier (long dash) are also shown. Thick lines indicate CHARMM partial charges, fine lines indicate GROMOS partial charges.

Although gA is charge neutral overall, the contribution of the permanent charge to the net potential energy profile is sensitive to the way in which this charged is distributed over the protein. There exist in the literature numerous different parameter sets for the distribution of charge on each amino acid. In Figure 2 we compare two different sets: the partial charges obtained with GROMOS [15] and with PARAM22/CHARMM. These two models present some difference in the charge distribution of the tryptophan side chains. We assume a dielectric coefficient of 20 for the protein, 2 for the lipid and 80 for the aqueous regions. The CHARMM partial charges result in a potential well almost 3 times deeper than that created by GROMOS. As a result, the net Na^+ PE profile for GROMOS is a barrier nearly 4k_BT high, while for CHARMM we have a double well of about 3k_BT. BioMOCA simulations show that under bias the channel described by GROMOS conducts Na^+ ions with a conductivity comparable to measurements. Indeed, the potential barrier for Cl^- is only ~3k_BT higher and under an applied bias of ~250 mV one could expect Cl^- to also permeate the channel. In fact, our model of gA with ε_p =20 and GROMOS charges does indeed conduct Cl^- if the ionic radius is set equal to that of Na^+. Thus we purport that ion size also plays a crucial role in gA conductivity. Since the pore radius (~2Å) is comparable to the ionic radii (r_+ = 0.95 Å, r_- = 1.8 Å), the probability for Na^+ to enter the channel is very low, and effectively zero for Cl^- (in several longer simulations lasting ~μs no Cl^- ions were ever observed inside the channel).

3 GRAMICIDIN: SIMULATIONS

We now present two example simulations of the gA channel *in situ* in a neutral lipid membrane of thickness 22 Å, using the 1MAG.pdb structure and partial charges taken from the GROMOS force field. The lipid, protein and electrolyte regions were assigned values of ε = 2, 20 and 80, respectively. Planar contacts parallel to the X-Y plane are included at either end of the domain so that a fixed bias voltage can be applied across the system. Na^+ and Cl^- scattering rates were determined from published ion diffusivities in bulk electrolyte [16]. The scattering rates are high, $\lambda_+ = 8.1\times10^{13}$ s^{-1} and $\lambda_- = 5.3\times10^{13}$ s^{-1} necessitating small time steps of 10fs. However, since the ions diffuse very slowly, the charge distribution does not change appreciably during one time step. Benchmark simulations in bulk electrolyte have shown that for such high scattering rates the field can be updated as infrequently as every few ps without degrading the ion-ion pair correlation function [10]. Here we solve Poisson's equation every 100 time steps (1ps). Figure 3 shows the Na^+ and Cl^- concentrations and potential, averaged over a 200ns simulation of 1M NaCl, as a function of position Z between the contacts. Both contacts were held at ground potential (zero bias). The

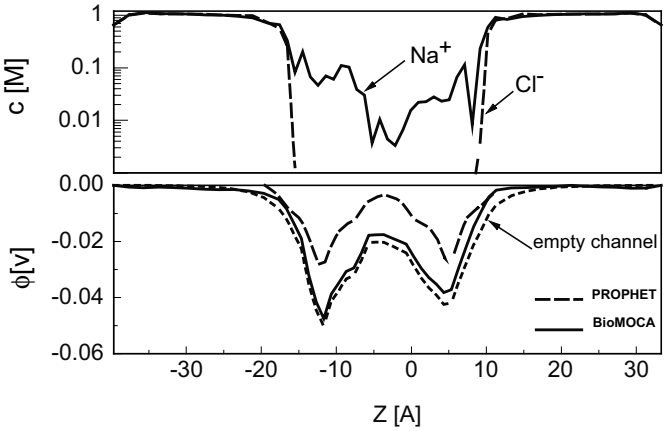

Figure 3. Time-averaged ion concentrations (top) and potential (bottom) as a function of z-position along the gA channel system, immersed in a 1M NaCl solution. No bias voltage was applied.

ion concentrations represent the average value in the X-Y plane, while the potential profile is taken along the center of the channel. The ion concentrations remain flat at ≈1M throughout the bath regions but inside the narrow pore region the Na^+ concentration drop by more than an order of magnitude while Cl^- is excluded altogether. The distribution of permanent fixed charge on the channel gives rise to an electrostatic potential distribution with two wells roughly $3k_BT/2$ deep, as shown by the solid line in the lower half of Figure 3. Also shown is the potential distribution in the absence of electrolyte (dotted line). The similarity between the two curves indicates that, at least over the period of observation, the fixed charge is not screened by the mobile ions. For comparison we have included the potential distribution calculated from steady-state continuum (drift-diffusion) theory on a finer (0.5 Å) mesh (dashed line). The assumption of average concentrations of point particles built into the continuum model allows a much higher concentration of ions of *both* species to enter the channel, resulting in partial screening of the fixed charge, as evidenced by the shallower potential wells.

The number of ions crossing the channel and the average Na^+ concentration inside the channel increases dramatically when a bias voltage is applied across the system. In Figure 4 we show the time-averaged Na^+ and Cl^- concentration and potential profiles with 250mV applied at the right contact. The simulation was run for 400 ns during which 10 Na^+ ions were detected crossing the channel from the right bath to the left. Though the applied field increases ion conduction, the average Na^+ concentration inside the channel is still an order of magnitude lower than in the baths − the channel presents a bottleneck to ion flow, causing almost all the applied potential to drop across the channel. In order to gauge the channel conductivity several channel simulations were performed with a 250mV bias and 1M NaCl in each bath. During the cumulative observation time of 26.3μs a total of 283 Na^+ ions crossed the channel, corresponding to a current of approximately

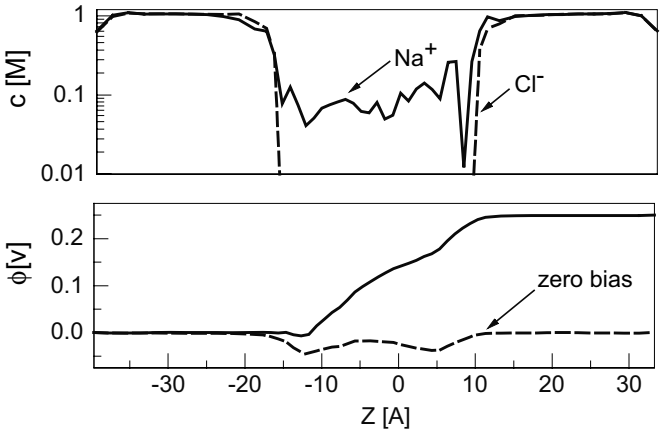

Figure 4. Time-averaged ion concentrations (top) and potential (bottom) as a function of z-position along the gA channel system, immersed in a 1M NaCl solution, under a bias voltage of 250 mV.

1.7 pA which compares well with single-channel current-voltage measurements [17].

ACKNOWLEDGMENTS

This work was partially supported by the National Science Foundation through the Network for Computational Nanotechnoogy Center, DARPA (contract SIMBIOSYS AF NA 0533) and the National Center for Supercomputing Applications. The authors are grateful to R. S. Eisenberg, B. Corry and E. Tajkhorshid for many useful discussions.

REFERENCES

[1] B. Hille, "Ionic Channels of Excitable Membranes" Sinauer Associates Inc., 1992.

[2] Saint, N., K.-L. Lou, C. Widmer, M. Luckey, T. Schirmer and J.P. Rosenbusch. J. Biol. Chem., **271**, 20676, 1996.

[3] Tajkhorshid, E., P. Nollert, M. Ø. Jensen, L. J. W. Miercke, J. O'Connell, R. M. Stroud, and K. Schulten. Science, **296**, 525, 2002.

[4] Ciccotti, G. and W.G. Hoover, eds. "Molecular-Dynamics Simulations of Statistical-Mechanical Systems", North Holland, 1986.

[5] B. Roux, Curr. Op. Struc. Biol.**12**, 182-189, 2002.

[6] Cardenas, A.E., R.D. Coalson and M.G. Kurnikova, Biophys. J., **79**, 80, 2000.

[7] T. A. van der Straaten, J. M. Tang, U. Ravaioli, R. S. Eisenberg and N. R. Aluru. J. Comp. Elec. **2**, 29-47, 2003.

[8] U. Hollerbach, D. Chen, W. Nonner and B. Eisenberg, Biophys. J., **76,** A205, 1999.

[9] T. A. van der Straaten, G. Kathawala and U. Ravaioli, J. Comp. Elec., in press, 2003.

[10] T.A. van der Straaten, G. Kathawala, Z. Kuang, D. Boda, D.P. Chen, U. Ravaioli, R.S. Eisenberg and D. Henderson, "Technical Proceedings of the 2003 Nanotechnology Conference and Trade Show", **3**, 447-451, 2003.

[11] C. N. Schutz and A. Warshel, Proteins: Structure, Function and Genetics, **44**,400, 2001.

[12] R. Pomes and B. Roux B, Biophys. J., **82**, 2304, 2002.

[13] S. Edwards, B. Corry, S. Kuyucak and S.-H. Chung, Biophys. J., **83**, 1348, 2002.

[14] B. Nadler, U. Hollerbach and R. S. Eisenberd, Phys. Rev. E., **68**, 21905, 2003.

[15] http://www.igc.ethz.ch/gromos/

[16] D.R. Lide, editor-in-chief, "CRC Handbook of Chemistry and Physics", CRC press, **5**-90, 1994.

[17] D. D. Busath, C. D. Thulin, R. W. Hendershot, L. R. Phillips, P.Maughan, C. D. Cole, N. C. Bingham, S. Morrison, L. C. Baird, R. J. Hendershot, M. Cotton, T. A. Cross, Biophys. J. , **75**, 2830, 1998.